ceramics

MDPI

Article

Usability of Cr-Doped Alumina in Dosimetry

Ernests Einbergs *, Aleksejs Zolotarjovs, Ivita Bite, Katrina Laganovska, Krisjanis Auzins, Krisjanis Smits and Laima Trinkler

Institute of Solid State Physics, University of Latvia, Riga LV-1063, Latvia
* Correspondence: eeinbergs@gmail.com

Received: 30 June 2019; Accepted: 19 August 2019; Published: 2 September 2019

Abstract: Dosimetry is a widespread material science field dealing with detection and quantification of ionizing radiation using electronic processes in materials. One of the main aspects that determines the performance of dosimeters is the type of defects the material contains. Crystalline lattice imperfections are formed around impurity ions, which may have a smaller or larger size, or different oxidation states compared to host ions. In this study, we show what effects Cr impurities have on the luminescent properties of alumina. Porous Al_2O_3: Cr microceramics synthesized using the sol-gel method showed a higher thermoluminescence response than a single crystal ruby. We have found that Cr_2O_3 concentration of 0.2 wt% was optimal; it yielded the highest X-ray luminescence and thermostimulated luminescence readout of all studied additive concentrations added to alumina during synthesis. Our results show that Cr doped alumina could potentially be used as a promising new material for dosimetry of ionizing radiation.

Keywords: dosimetry; alumina; chromium; sol-gel; Al_2O_3: Cr

1. Introduction

Personal and industrial dosimeters provide a possibility to determine the radiation dose emitted by ionizing sources and radioactive materials. The technology is largely used by medical staff, atomic reactor maintainers, border control and scientists in areas where the absorbed dose must be controlled due to increased risk of developing harmful tumors and other injuries when working with ionizing radiation [1–3].

The best known and widely used dosimeter material on alumina basis is carbon-doped aluminum oxide Al_2O_3 : C (TLD-500) (band gap > 6 eV), which was proposed as a highly sensitive TL (thermoluminescent) and OSL (optically stimulated luminescence) material for personal dosimetry [4]; it is now commercially available as a TL and OSL dosimeter (Landauer, Inc., Glenwood, IL, USA). Its main application is in OSL dosimetry for medicine, such as radiotherapy, radiodiagnostics, as well as heavy charged particle dosimetry [5]. Although it has very attractive properties such as high sensitivity, stable signal at RT (room temperature) and a linear response over a wide range of doses (up to 50 Gy), this material shows disadvantages such as dependence of TL response on heating rate and overresponse to low-energy X-rays due to the effective atomic number—11.28. As a personal dosimeter, Al_2O_3:C is useful in the dose range 10 μGy–10 Gy but is not suitable at higher doses.

Efforts were undertaken to find other alumina-based dosimeter materials using different dopants. Some results were not as promising as others—several powdered doped Al_2O_3 samples produced by solution combustion method were characterized for TL and OSL properties [6]; however, they did not demonstrate attractive dosimeter properties. At the same time, Japanese researchers have found that doping with Cr enhances sensitivity and the fading characteristics of alumina, demonstrated in X-ray imaging, which makes this material suitable for two-dimensional TL slab dosimeters for robotic radiosurgery systems [7]. As shown in [8] doping of nanopowdered Al_2O_3 with chromium makes it

sensitive to higher γ-ray doses (100 Gy–20 kGy without saturation). Such properties might open novel application areas for Al_2O_3: Cr , such as radiation sterilization dosimetry and dealing with high doses during the irradiation of food products, seeds, medical instruments and agents.

Alumina has multiple phases, but in comparison to other alumina phases, the alpha phase is chemically inert and has a considerable hardness. It is also the most heat resistant phase, stable up to a temperature of 2051 °C; at higher temperatures it melts [9–12].

The most popular and widely used method for studying dosimetric properties is thermostimulated luminescence (TL). Ionizing radiation (in this study, X-rays were used) excites electrons from their ground level to the conduction band and this is followed by charge carriers geting trapped by the defects in the crystalline structure. Additional energy is necessary to release the charge carriers from the traps and to stimulate their recombination, thus causing the emission of a photon. The number of photons (registered luminescence intensity) correlates with the number of the trapped charge carriers, which in turn correlates with the absorbed radiation dose [13].

Dosimeters must exhibit a linear correlation between absorbed radiation dose and TL response. In this article, we study Cr-doped alpha alumina as a potential material for a high dose dosimeter. The search for the optimal Cr_2O_3 concentration during the sol-gel synthesis of Al_2O_3 and study of the dosimetric properties of the acquired Cr-doped alumina is presented. Comparison of luminescence intensity is done between microceramic powder and a ruby single crystal.

2. Materials and Methods

2.1. Materials

Aluminum nitrate nanohydrate $(Al(NO_3)_3{\cdot}9H_2O$, purity 99.6%; VWR Prolabo Chemicals, Singapore); and chromium (III) oxide (Cr_2O_3) were used as starting materials. Citric acid ($C_6H_8O_7$, purity 99.5%) and ethylene glycol ($HO(CH_2)_2OH$, purity 99%) were used as chelating and polymerizable agents, and both were purchased from Sigma Aldrich. Nitric acid (HNO_3, assay 65%) (Sigma Aldrich, Saint Louis, MO, USA) was used to dissolve Cr_2O_3. Analytical grade chemicals were used without any further purification.

2.2. Synthesis of Non-Doped and Cr-Doped Al_2O_3 Microceramic Powder

Pure and Cr-doped alumina samples were synthesized using the sol-gel polymerized complex method, which was also used in our previous work [14]. Cr-doped alumina samples were prepared with varying concentrations (0.1, 0.2, 0.3, 0.35, 0.4, 0.7, 1 and 1.5 wt%) of the Cr_2O_3. The molar ratio of metal ions, citric acid, and ethylene glycol was 1:1:4, respectively. Also, an appropriate amount of deionized water was added so that the molar concentration of all metals ions in the solution would be 0.2 M. When the necessary gel consistency was obtained, it was heated in an open oven at 400 °C for 2 h for nitric oxide elimination, and as a result a black powder was obtained. After synthesis, the obtained samples were calcined at 1400 °C for 4 h. In the end, white and pink powders were obtained.

2.3. Characterization Techniques

The crystalline phases of pure and Cr_2O_3 doped Al_2O_3 samples after heat treatment were characterized by X-ray powder diffraction (XRD) using a PANalytical X'Pert Pro diffractometer. Cu Kα radiation (1.5418 Å) was used by setting the cathode voltage to 45 kV and current to 40 mA. Morphology and chemical composition of the pure and Cr_2O_3 doped Al_2O_3 samples were characterized by scanning electron microscopy (SEM) using Tescan Lyra equipped with an energy dispersive X-ray (EDX) spectrometer operated at 15 kV. Before the examination, the samples were coated with a gold layer.

XRL (X-ray luminescence) and TL (thermostimulated luminescence) spectra were acquired using an ANDOR SR-303I-B monochromator with a 150 L/mm diffraction grating and a blaze wavelength of 800 nm. The monochromator was coupled with an ANDOR DU401A-BV CCD camera and an ANDOR SOLIS data logger. To avoid oxygen ionizing in the measurement chamber and the heater oxidizing

during measurements, a vacuum pump ILMVAC GmbH CD 2015 was used, which provided a vacuum greater than 10^{-5} Torr.

XRF (X-ray fluorescence) measurements were performed using an EAGLE Probe III X-ray fluorescence spectrometer. The X-ray lamp was set to a current of 10 A and a voltage of 40 kV. Rays were focused on a circular area with a diameter of 200 μm. Since dopant concentrations were small, the XRF spectrometer was operated at the detection limit. This meant that the measurement errors were rather large, as was determined by repeatedly measuring the same sample in different surface locations and calculating the average value and standard deviation. Measurement error was determined for one sample and the authors assume that it will stay consistent with all other samples in the series.

3. Results

3.1. XRD Measurements

Results of the X-ray diffraction measurements displayed in Figure 1 show that all samples contain the same alpha alumina phase [15,16]. Since no changes in the X-ray diffraction pattern are noticeable, one can assume that Cr_2O_3 at the studied concentrations does not cause any major disruptions in the crystalline lattice of the host matrix.

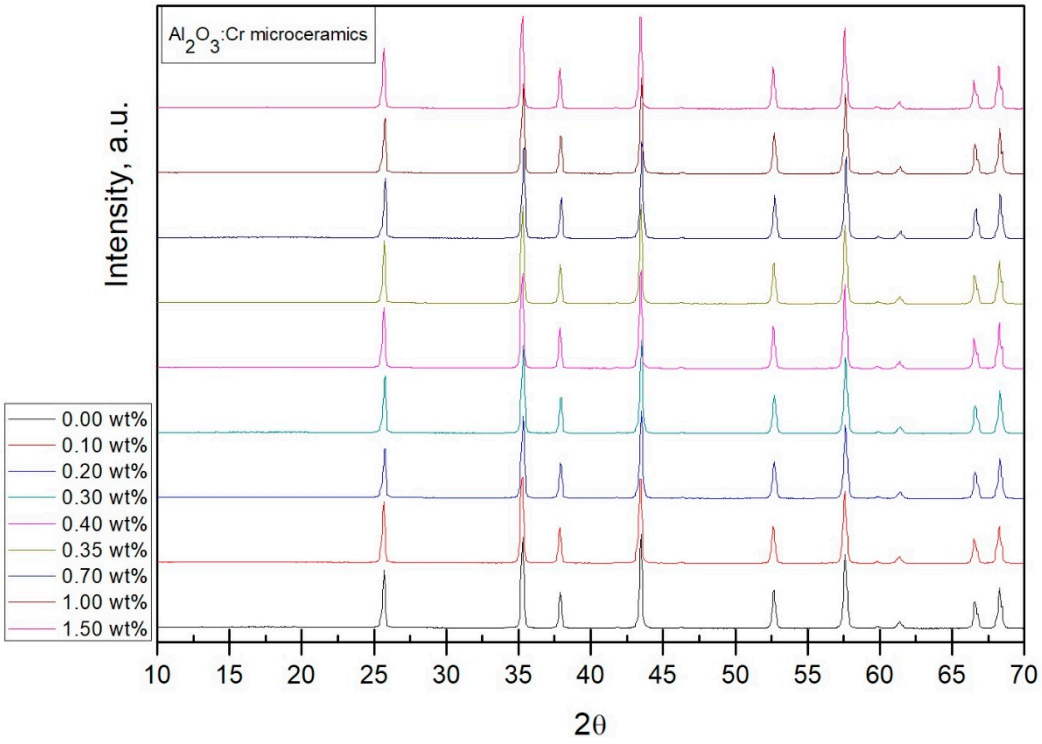

Figure 1. XRD results for all 9 samples with varying chromium concentrations.

3.2. Composition Analysis

Comparisons between the initial and post-synthesis Cr_2O_3 concentrations were made using an EDX and XRF and results can be observed in Figure 2. The main conclusions that can be drawn are that although the detected concentration grows by increasing the initial concentration, the efficiency at which Cr_2O_3 incorporates into the crystal lattice is not straightforward and has to be further studied. The obtained average EDX readouts are closer to the initially added Cr concentrations than the XRF results. This might be explained by the technological differences in measurement devices. Since the area studied in XRF measurements is larger, it might lead to erroneous results due to the sample inhomogeneity.

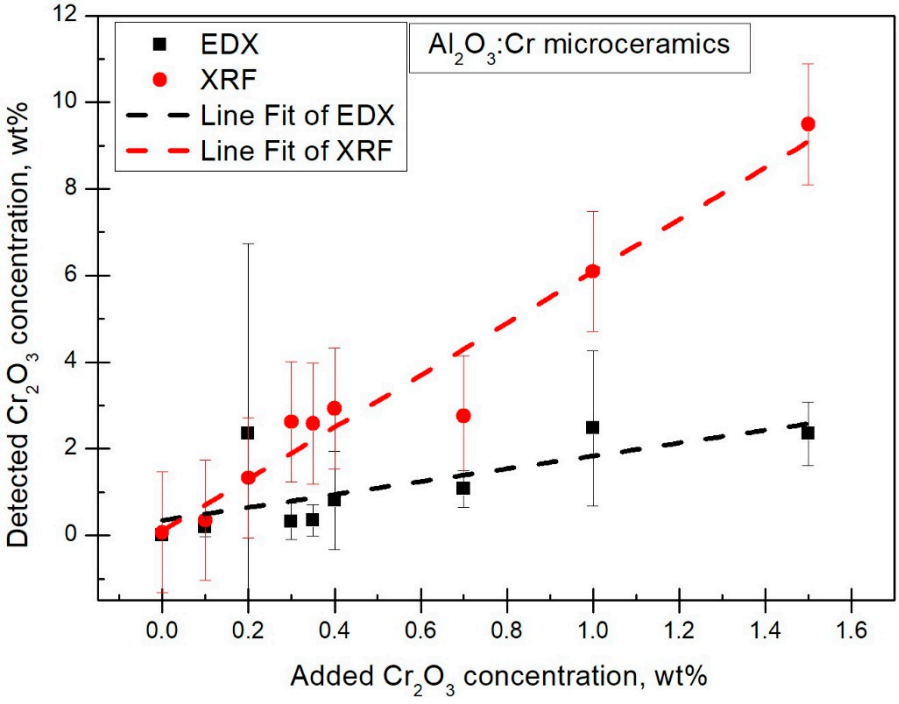

Figure 2. EDX and XRF results.

3.3. SEM Measurements

The results of the SEM measurements are shown in Figure 3. From these results, we propose that a 4 h long heat treatment at 1400 °C is enough for nanoparticles to start joining together, forming porous microceramics. These results suggest that a lower temperature and shorter heat treatment duration could create nanoparticles if a way was found to eliminate all organic matter traces after synthesis with such conditions.

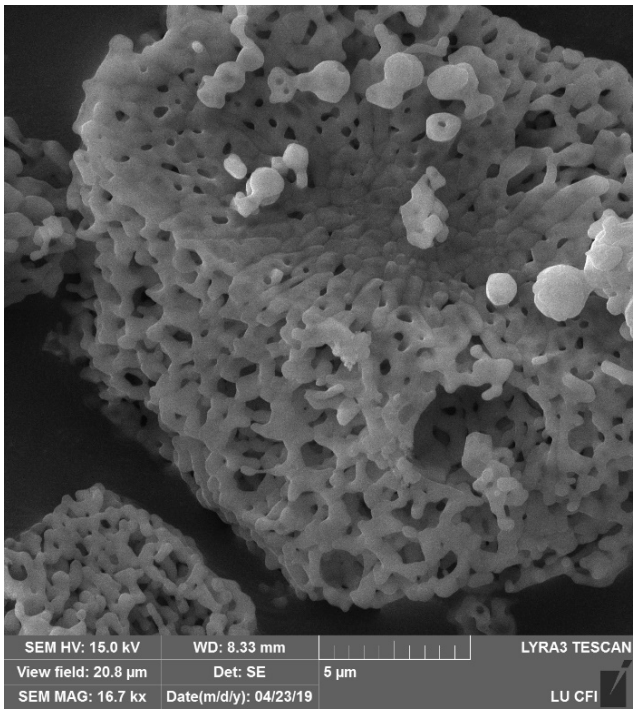

(**a**)

Figure 3. *Cont.*

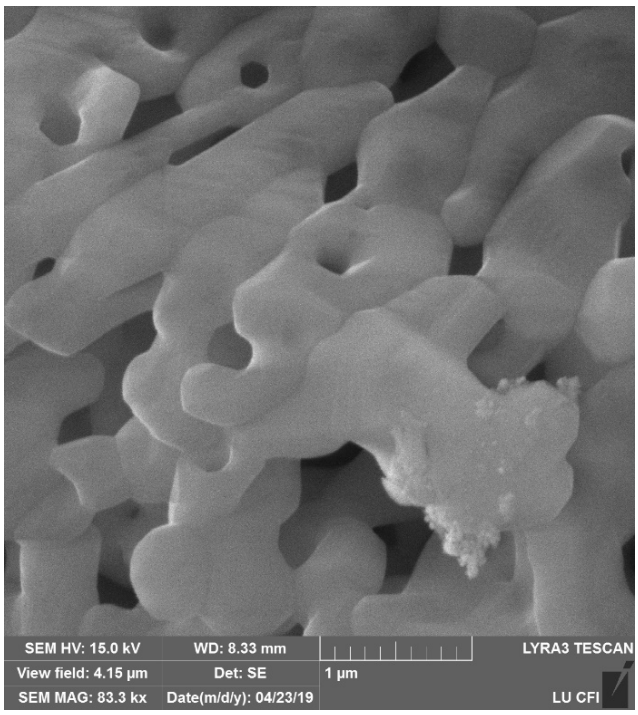

(**b**)

Figure 3. SEM results. (**a**) One microparticle. (**b**) The same particle with a higher zoom; the traces of nanoparticles can be observed.

3.4. Luminescence Measurements

The X-ray luminescence spectra were registered for all microceramics samples. A ruby single crystal was used as a reference. The results can be seen in Figure 4. Cr^{3+} specific lines R_1, R_2 and N were observed with the respective wavelengths being 694.7, 693.3 and 704 nm [17]. R_1 and R_2 arise from electron excitation from $^4A_2$ to $^4T_2$ and $^4T_1$ state, where energies are about 2.2 and 3.0 eV above the ground state. Electrons relax to ^4E state by generating phonons and afterward return to $^4A_2$ by emitting photons with wavelengths 694.7 and 693.3 nm. The weaker N line around 704 nm arises from the interaction of two closely located Cr ions, and the broader emission line around 715 nm is assigned to Cr ion cluster interaction [17].

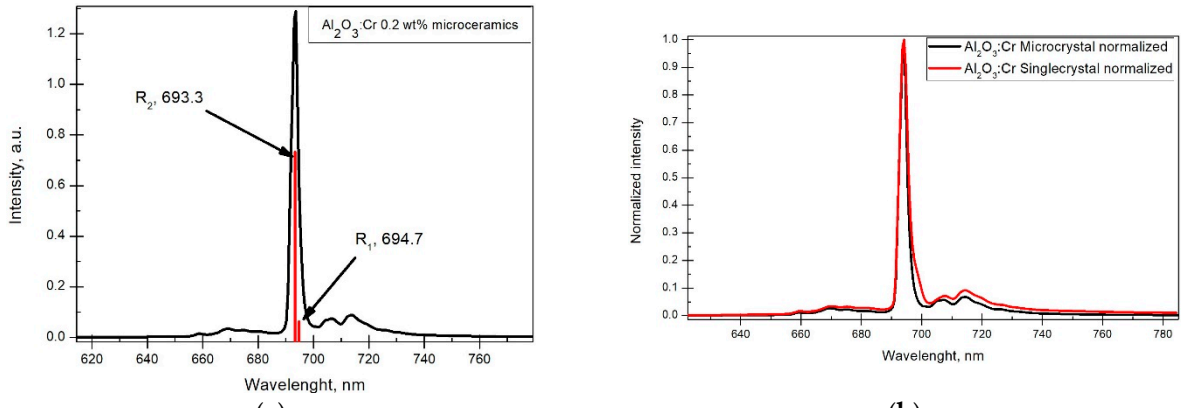

(**a**) (**b**)

Figure 4. X-ray excited luminescence spectra for (**a**) Al_2O_3: Cr microparticles; (**b**) normalized Al_2O_3: Cr microparticles and ruby single crystal. No notable differences can be observed between two sample spectra. In both cases, no emission lines were registered from 300 nm to 650 nm.

3.5. Concentration Optimization

By analyzing the relation between the added Cr_2O_3 concentration and the luminescence intensity (Figure 5), a conclusion was drawn that the optimal Cr concentration could be found in the range of 0.2 to 0.3 wt%. To get a more accurate optimal Cr_2O_3 concentration for dosimetric purposes, the integral intensity was determined. Error bars in Figure 5 represent the measurement uncertainty that arises from our optical systems, which is estimated to be 10% of the total intensity.

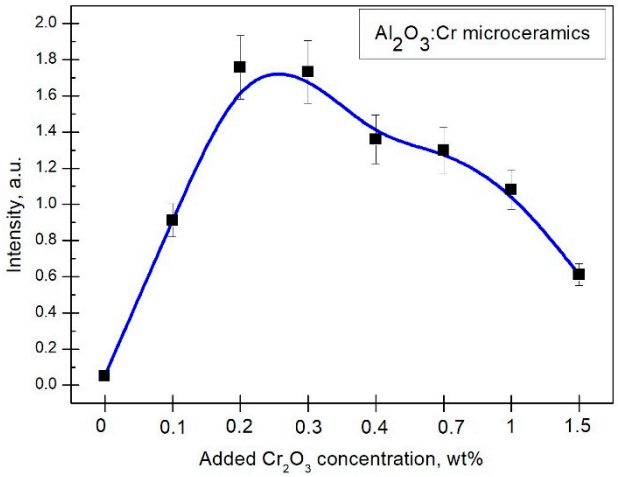

Figure 5. X-ray luminescence intensity dependence on added chromium concentration of Al_2O_3: Cr microceramics.

3.6. TL Measurments

TL measurements were conducted from 20 °C to 450 °C. To determine the optimal concentration, a constant irradiation time of 30 min and a 10 min delay time after irradiation was used to avoid registering sample afterglow. An example is shown in Figure 6. As the experimental setup allows the measuring of both the temperature and wavelength dependence of luminescence simultaneously, the analysis of both TL and spectral distribution in TL peaks is presented. The spectra for the main TL peaks are presented in Figure 6b. The glow peak around 120 °C was not studied due to difficulties determining the exact maximum of the peak. All observed glow peaks arise from charge traps with different depths. Spectra in Figure 6b show that the main contributors to thermostimulated luminescence are Cr^{3+} ions. Two broad lines on each side of the previously mentioned R lines (Figure 4) were observed, and their intensities relative to the R line increased at higher temperatures. In other studies, these are mentioned as vibrational sidebands of R lines [18].

The relation between integral TL intensity and added Cr_2O_3 concentration can be seen in Figure 7. A conclusion can be made that the optimal Cr_2O_3 concentration is around 0.2 wt%. Error bars represent standard deviation between 3 consecutive measurements and the black line connecting points serves for visual clarity only.

Both rise and fall in TL intensity can be explained by an increase in Cr_2O_3 concentration. A rise could be due to an increase in luminescence or recombination centers in the crystal lattice. The steep fall could be explained by an effect known as concentration quenching, where photon absorption rises more quickly than emission as the Cr_2O_3 concentration increases [19].

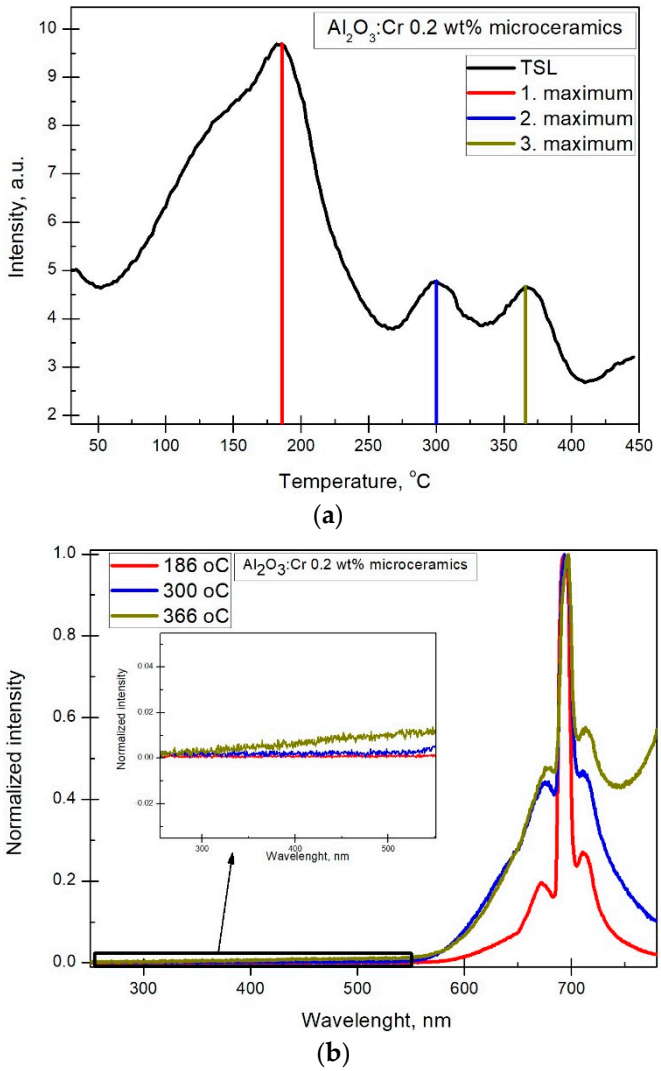

Figure 6. (**a**) Single TL measurement of Al_2O_3: Cr with 0.2 wt% Cr_2O_3. (**b**) Al_2O_3: Cr with 0.2 wt% Cr_2O_3 luminescence spectra of the 3 corresponding peaks. Insert shows that no meaningful signal was registered from 250 to 550 nm.

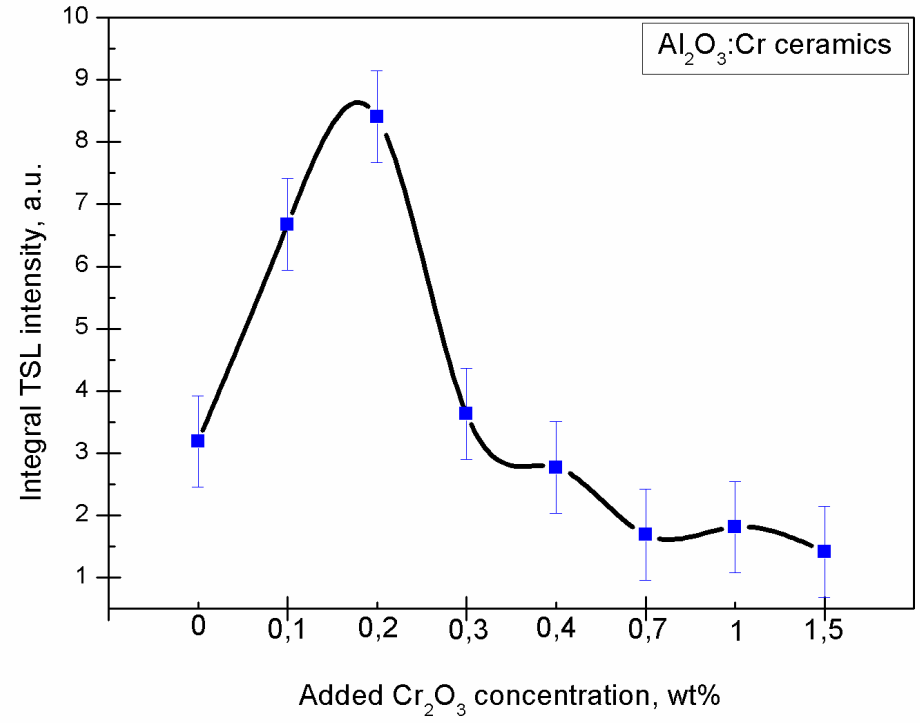

Figure 7. Relation between integral TL intensity and added chromium concentration for microceramics.

3.7. Dosimetric Properties

Based on the previous conclusions, the sample with 0.2 wt% Cr_2O_3 was investigated further. TL measurements were repeated in the same conditions: temperature range and the delay time before irradiation and actual measurements were held constant. The only varying parameter was the irradiation time. Results for all three TSL peaks can be seen in Figure 8. To create the full dosimetric curve, six irradiation times were chosen: 1; 5; 15; 30; 60 and 90 min respectively [20,21]. To determine which maximum was the best for dosimetric applications, a separate measurement was made to check the impact of TL fading; this sample was irradiated for 15 min, and then a 60 min pause was taken before the TL readout. Results in Figure 9 show that the first maximum cannot be reliably used for intended purposes, because it demonstrates essential fading. The 10% measurement uncertainty caused the second and third TSL peaks to appear to have a higher readout after the 60 min delay than it had after 15 min.

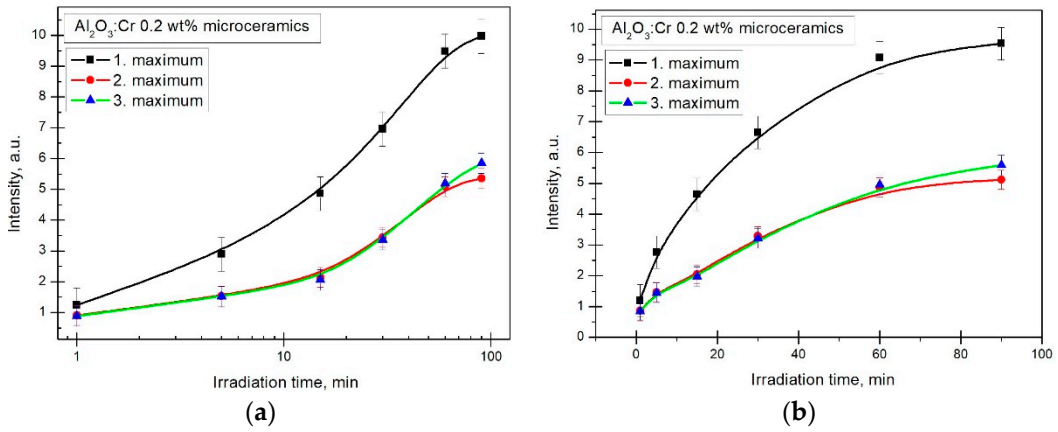

Figure 8. TL intensity dependence on irradiation time. (**a**) Results with a logarithmic time scale to illustrate that saturation and undersaturation has been achieved and (**b**) with a linear time scale to provide a more intuitive view.

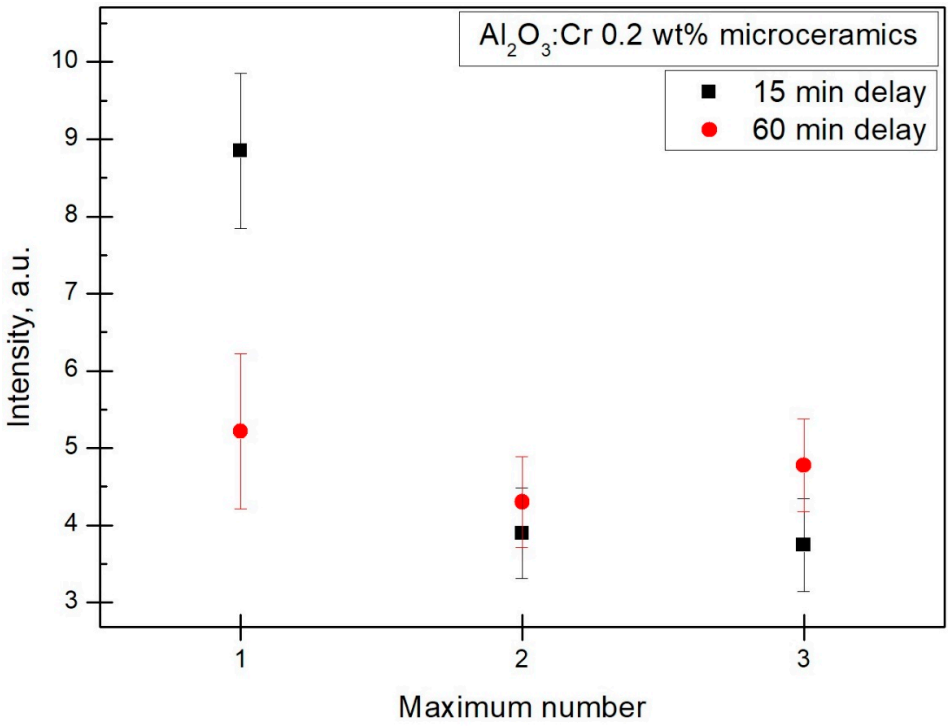

Figure 9. TL peak intensity variance caused by increased delay time in Al_2O_3: Cr with 0.2 wt% Cr_2O_3.

Relying on Figure 9, the linearity was determined only for the third peak. However, it is highly likely that the second peak would have the same linearity as the points almost overlap. Figure 10 shows that the third peak displays a linear response to irradiation time from 1 to 60 min. Points matched in a line with a reduced Chi–Sqr value of 0.34.

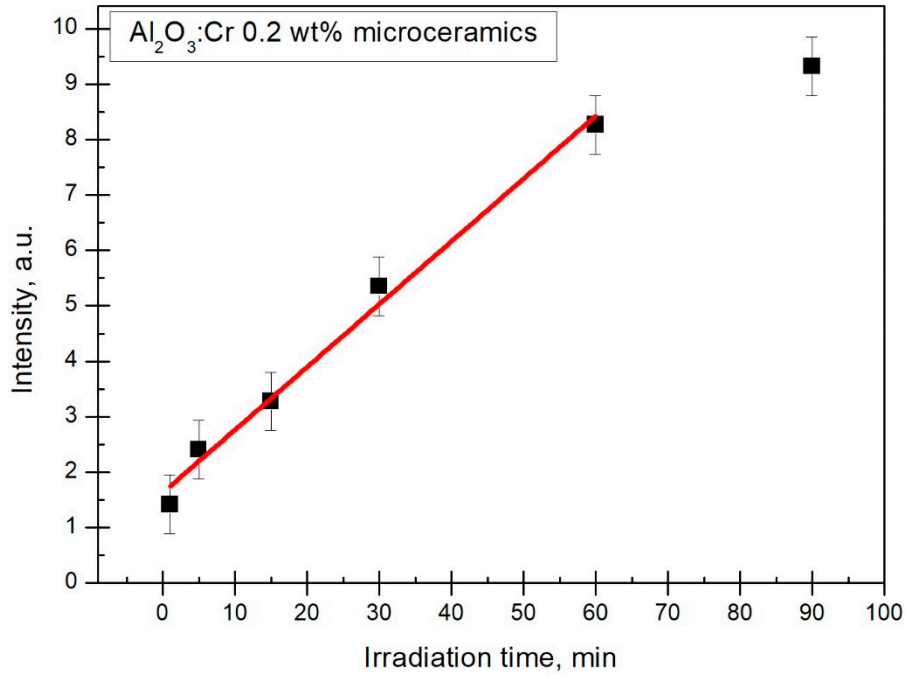

Figure 10. TL intensity dependence on irradiation time with a linear fit for Al_2O_3: Cr with 0.2 wt% Cr_2O_3 (only third peak is shown to avoid visual clutter).

4. Discussion

Comparison with widely used carbon-doped alumina is rather difficult. For theoretical purposes, an estimation was made using RadPro Calculator 3.26. Inserting our measurement parameters yielded a dose rate of about 99 Gy min^{-1}. That means that Cr_2O_3-doped alumina has a linear response from around 100 Gy to 5 kGy. Literature shows that carbon-doped alumina has a linear range from 10^{-6} to 1 Gy [4]. This means that Cr_2O_3-doped alumina could be applied as a high dose dosimeter, which could then be used in reactors or border control as an onboard equipment regulator.

For optimal dose response and sensitivity, the whole TL spectrum should be integrated when determining the ionizing radiation dose absorbed by the material, instead of only individual peak intensities. Integral value would provide maximal information without unnecessary loss of information, but a correction must be determined which considers fading rate, temperature at which the sample was stored and the amount of light the sample absorbed while in use as a passive dosimeter.

To determine the dose response, the irradiation time was varied. Longer irradiation leads to a higher absorbed dose by the sample, but also to the higher absolute impact of fading of the TL response. Divergence from linearity could be caused by fading under irradiation which was not taken into account during linearity analysis. Material could possess a wider linear response dose range than the one reported in this study, which could be used as a basis for further exploration of Cr_2O_3 doped Al_2O_3.

5. Conclusions

Study of dosimetric properties of Cr_2O_3-doped alumina microceramic shows that its TL response displayed a promising linearity in the performed measurement X-ray dose range, and the estimations imply that this material is suitable for detection of rather high doses of ionizing radiation (100 Gy to 5 kGy). The physical and chemical properties of the material, as well as its manufacturing cost, make it a good candidate for potential use as a dosimeter.

In future research, time dependence should also be studied over a considerably longer period. Single crystalline Cr_2O_3-doped alumina should also be explored in more detail. Cr-doped microceramic powder showed some features that are promising for dosimetry applications, however, the noticeable fading raises several concerns.

Author Contributions: E.E. carried out most of the measurements, performed data analysis, and is the main contributor to this article. A.Z. assisted in measurements and data interpretation. I.B. synthesized the samples and performed XRD measurements. K.L. and K.A. assisted in data analysis and proof-reading of the paper. K.S. and L.T. assisted in writing the paper and supervised the direction for the research.

Funding: Financial support provided by Scientific Research of Luminescence Mechanisms and Dosimeter Properties in Prospective Nitrides and Oxides Using TL and OSL Methods LZP FLPP Nr. LZP-2018/1-0361 realized at the Institute of Solid State Physics, University of Latvia is greatly acknowledged.

Conflicts of Interest: The authors declare no conflict of interest.

References

1. Einstein, A.J.; Henzlova, M.J.; Rajagopalan, S. Estimating Risk of Cancer Associated with Radiation Exposure From 64-Slice. *JAMA* **2007**, *298*, 317–323. [CrossRef] [PubMed]
2. Cardis, E.; Gilbert, E.S.; Carpenter, L.; Howe, G.; Kato, I.; Armstrong, B.K.; Beral, V.; Cowper, G.; Douglas, A.; Fix, J.; et al. Effects of Low Doses and Low Dose Rates of External Ionizing Radiation: Cancer Mortality among Nuclear Industry Workers in Three Countries. *Radiat. Res.* **2006**, *142*, 117–132. [CrossRef]
3. Duncan, J.R.; Lieber, M.R.; Adachi, N.; Wahl, R.L. DNA Repair After Exposure to Ionizing Radiation Is Not Error-Free. *J. Nucl. Med.* **2018**, *59*, 348. [CrossRef] [PubMed]
4. Akselrod, M.S.; McKeever, S.W.S. A Radiation Dosimetry Method Using Pulsed Optically Stimulated Luminescence. *Radiat. Prot. Dosim.* **1999**, *81*, 167–176. [CrossRef]
5. Yukihara, E.G.; McKeever, S.W.S. Optically stimulated luminescence (OSL) dosimetry in medicine. *Phys. Med. Biol.* **2008**, *53*, 351–379. [CrossRef] [PubMed]

6. Yukihara, E.G.; Milliken, E.D.; Oliveira, L.C.; Orante-Barrón, V.R.; Jacobsohn, L.G.; Blair, M.W. Systematic development of new thermoluminescence and optically stimulated luminescence materials. *J. Lumin.* **2013**, *133*, 203–210. [CrossRef]
7. Yanagisawa, S.; Shinsho, K.; Inoue, M.; Koba, Y.; Matsumoto, K.; Ushiba, H.; Andoh, T. Applicability of two-dimensional thermoluminescence slab dosimeter based on Al_2O_3: Cr for the quality assurance of robotic radiosurgery. *J. Lumin.* **2018**, *30*, 1591–1598.
8. Akselrod, V.I.; Kortov, M.S.; Kravetsky, V.S.; Gotlib, D.J. Highly Sensitive Thermoluminescent Anion-Defective Alpha-Al_2O_3: C Single Crystal Detectors. *Radiat. Prot. Dosim.* **1990**, *32*, 15–20.
9. Davis, K. Material Review: Alumina. *Sch. Dr. Stud. Eur. Union J.* **2010**, *3*, 109–115.
10. Cunha, G.D.; Romão, L.P.C.; Macedo, Z.S. Production of alpha-alumina nanoparticles using aquatic humic substances. *Powder Technol.* **2014**, *254*, 344–351. [CrossRef]
11. Lamouri, S.; Hamidouche, M.; Bouaouadja, N.; Belhouchet, H.; Garnier, V.; Fantozzi, G.; Trelkat, J.F. Control of the γ-alumina to α-alumina phase transformation for an optimized alumina densification. *Boletín Soc. Española Cerámica Vidr.* **2017**, *56*, 47–54. [CrossRef]
12. Chandran, C.V.; Kirschhock, C.E.A.; Radhakrishnan, S.; Taulelle, F.; Martens, J.A.; Breynaert, E. Alumina: Discriminative analysis using 3D correlation of solid-state NMR parameters. *Chem. Soc. Rev.* **2019**, *48*, 134–156. [CrossRef] [PubMed]
13. McKeever, S.W.S. *Thermoluminescence of Solids*; Cambridge University Press: Cambridge, UK, 1983.
14. Laganovska, K.; Bite, I.; Zolotarjovs, A.; Smits, K.; Ofelt, J. Niobium enhanced europium ion luminescence in hafnia nanocrystals. *J. Lumin.* **2018**, *203*, 358–363. [CrossRef]
15. Sadabadi, H.; Aftabtalab, A.; Zafarian, S.; Shaker, S.; Ahmadipour, M.; Rao, K.V. High purity Alpha Alumina nanoparticle: Synthesis and characterization. *Int. J. Sci. Eng. Res.* **2013**, *4*, 1593–1596.
16. Chargui, F.; Hamidouche, M.; Belhouchet, H.; Jorand, Y.; Doufnoune, R.; Fantozzi, G. Mullite fabrication from natural kaolin and aluminium slag. *Boletín Soc. Española Cerámica Vidr.* **2018**, *57*, 169–177. [CrossRef]
17. Bhardwaj, D.M.; Jain, D.C.; Rao, K.V.R.; Kumar, R.; Singh, F.; Gupta, R.P. Photoluminescence and atomic force microscopic studies on pre- and post-irradiated ruby with Ni^{6+} ion. *Nucl. Instrum. Methods Phys. Res. Sect. B Beam Interact. Mater. At.* **2004**, *222*, 533–537. [CrossRef]
18. Trinkler, L.; Berzina, B.; Jakimovica, D.; Grabis, J.; Steins, I. UV-light induced luminescence processes in Al_2O_3 bulk and nanosize powders. *Opt. Mater.* **2010**, *32*, 789–795. [CrossRef]
19. Harris, D.C. *Quantitative Chemical Analysis*, 9th ed.; W. H. Freeman: New York, NY, USA, 2015; Volume 407.
20. Di Veroli, G.Y.; Fornari, C.; Goldlust, I.; Mills, G.; Koh, S.B.; Bramhall, J.L.; Richards, F.M.; Jodrell, D.I. An automated fitting procedure and software for dose-response curves with multiphasic features. *Sci. Rep.* **2015**, *5*, 14701. [CrossRef] [PubMed]
21. Kalita, J.M.; Chithambo, M.L. The effect of annealing and beta irradiation on thermoluminescence spectra of α-Al_2O_3: C, Mg. *J. Lumin.* **2018**, *196*, 195–200. [CrossRef]